Geophys. J. Int. (2002) **150,** 809–819

Motion of the Philippine Sea plate consistent with the NUVEL-1A model

Shao Xian Zang,[1] Qi Yong Chen,[1,*] Jie Yuan Ning,[1] Zheng Kang Shen[2] and Yong Gang Liu[1]

[1]*Department of Geophysics, Peking University, Beijing* 100871, *China. E-mail: sxzang@pku.edu.cn*
[2]*Department of Earth Sciences, University of California, Los Angeles, CA, USA*

Accepted 2002 April 12. Received 2002 April 3; in original form 2001 June 5

SUMMARY

We determine Euler vectors for 12 plates, including the Philippine Sea plate (PH), relative to the fixed Pacific plate (PA) by inverting the earthquake slip vectors along the boundaries of the Philippine Sea plate, GPS observed velocities, and 1122 data from the NUVEL-1 and the NUVEL-1A global plate motion model, respectively. This analysis thus also yields Euler vectors for the Philippine Sea plate relative to adjacent plates. Our results are consistent with observed data and can satisfy the geological and geophysical constraints along the Caroline (CR)–PH and PA–CR boundaries. The results also give insight into internal deformation of the Philippine Sea plate. The area enclosed by the Ryukyu Trench–Nankai Trough, Izu–Bonin Trench and GPS stations S102, S063 and Okino Torishima moves uniformly as a rigid plate, but the areas near the Philippine Trench, Mariana Trough and Yap–Palau Trench have obvious deformation.

Key words: earthquake slip vectors, Euler vector, intraplate deformation, Philippine Sea plate, relative plate motion.

INTRODUCTION

The Philippine Sea plate, proposed as a distinct plate at the early stage of plate motion theory (Morgan 1971; Le Pichon *et al.* 1976) plays a special role in the tectonic history of the western Pacific and eastern Eurasian continent. However, its motion relative to the surrounding plates is difficult to determine because its boundaries consist primarily of subduction zones rather than accreting boundaries where relative motion rates can be determined and transform boundaries where relative motion azimuths can be determined more accurately than from earthquake slip vectors (Chase 1972, 1978; Minster *et al.* 1974; Minster & Jordan 1978; Seno *et al.* 1993).

Before the availability of space geodetic data, only slip vectors of thrust earthquakes along the subduction boundaries of the Philippine Sea plate could be used to constrain its motion. This situation caused at least three sources of uncertainties. First, the backarc spreading and the deformation of overriding plate, such as the spreading of Mariana Trough and Okinawa Trough (Imanishi *et al.* 1996), and strike-slip faulting within the overriding plate, such as that occurring at the Philippine Fault (PF) and the Median Tectonic Line (MTL) in SW Japan, can make the azimuths of earthquake slip vectors differ from the relative plate motion (Karig 1975; Ranken *et al.* 1984; Fitch 1972; Jarrard 1986; DeMets *et al.* 1990; Seno *et al.* 1993; Zang *et al.* 1994). Secondly, some small collisional zones around the Philippine Sea plate, such as in Taiwan, Caroline Ridge–Yap arc and Izu arc-Central Honshu, make earthquake focal mechanisms more complicated (Seno *et al.* 1993). Finally, it is uncertain whether the northern boundary of the Philippine Sea plate is adjacent to the Eurasian plate, the North American plate, or a distinct Okhotsk plate (Seno *et al.* 1993, 1996; Wei & Seno 1998). These problems must be borne in mind and data must be selected with caution before we determine the Euler vector of the Philippine Sea plate with interplate earthquake slip vectors.

Many researchers have discussed or obtained Euler vectors of the Philippine Sea plate with earthquake slip vectors (Seno 1977; Chase 1978; Minster & Jordan 1978; Karig 1975; Ranken *et al.* 1984; Huchon 1986), or discussed the constraining conditions (Weissel & Anderson 1978). Seno *et al.* (1993) discussed the deficiencies in previous studies and obtained Euler vectors for the Philippine Sea plate related to the adjacent major plates such as Eurasia (EU), Pacific (PA) and the small Caroline (CR) plate by using 11 and 16 earthquake slip vectors at Nankai Trough–Ryukyu Trench along the PH–EU boundary and at Izu–Bonin Trench along the PH–PA plate boundary, respectively, subject to the constraint of an EU–PA motion predicted by the global relative plate motion model NUVEL-1. Seno *et al.*'s result is now most widely used, but the data constraining motion of the Philippine Sea plate are still sparse, and are particularly lacking in the rate data.

*Now at: Department of Geological Sciences, Northwestern University, Evanston, IL 60208, USA.

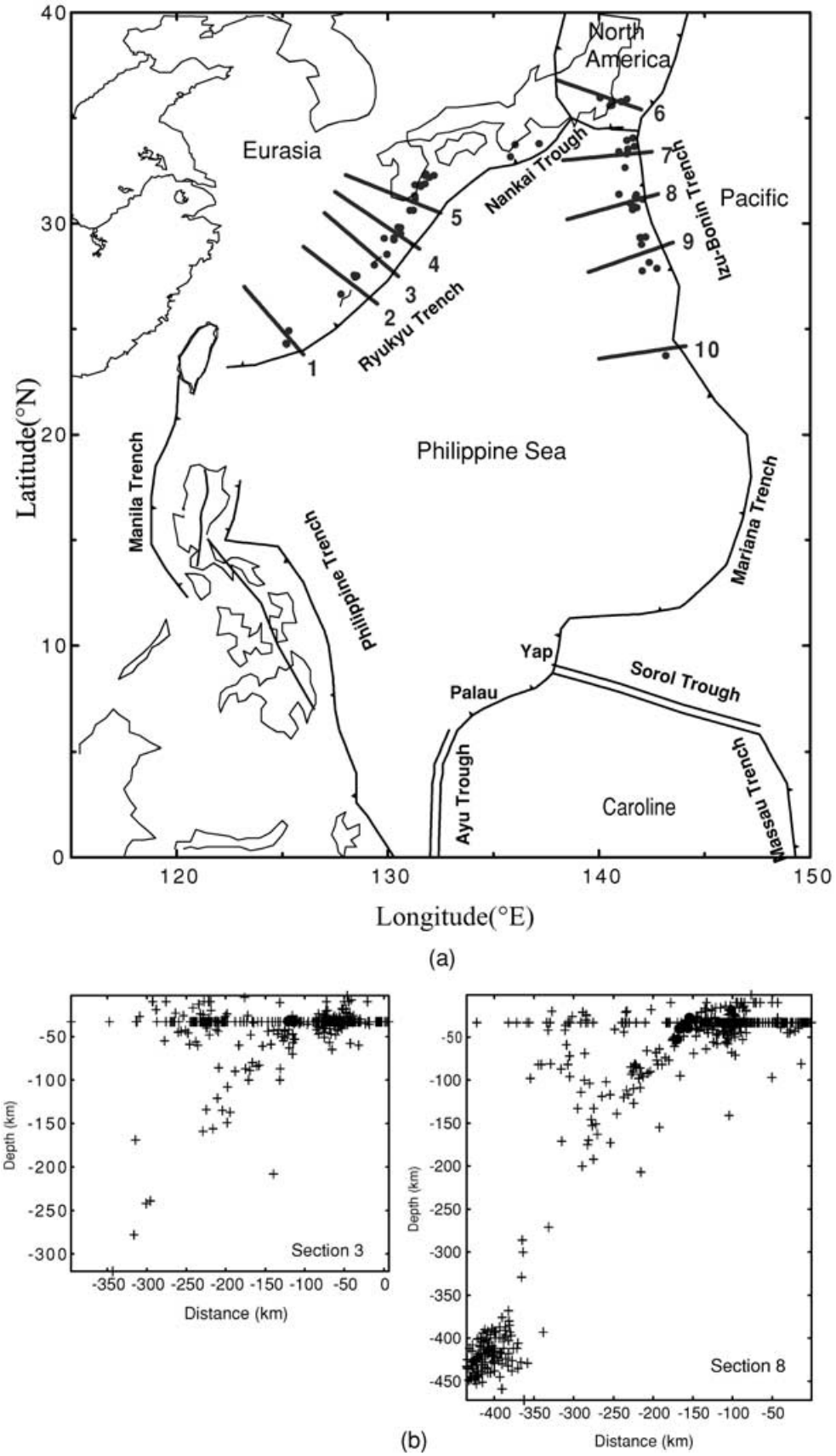

Figure 1. (a) Positions of epicentres of earthquake chosen to determine the slip vectors in this study and the cross-sections used to choose the earthquakes. •, epicentres of earthquakes that meet the three conditions (see text);—with number, cross-sections. (b) Two cross-sections in (a). The crosses denote the earthquakes in the cross-sections, and the black dots are earthquakes used in this study.

Table 1a. Data at the PH–EU boundary (Nankai Trough–Ryukyu Trench).

Lat. (°N)	Lon. (°E)	Obs. (deg)	σ (deg)	IMP	Pre. (deg)	Source or reference
33.70	136.05	−54.0	10.0	0.029	−43.7	Seno *et al.* (1993)
33.13	135.84	−50.0	10.0	0.028	−44.5	Seno *et al.* (1993)
32.31	131.83	−48.0	15.0	0.012	−42.9	Seno *et al.* (1993)
32.26	131.78	−49.0	10.0	0.027	−42.9	Seno *et al.* (1993)
32.24	132.21	−54.0	15.0	0.012	−43.2	Seno *et al.* (1993)
32.23	131.78	−48.0	10.0	0.027	−43.0	Seno *et al.* (1993)
32.15	131.98	−48.0	15.0	0.012	−43.2	Seno *et al.* (1993)
31.84	131.80	−51.4	20.0	0.006	−43.5	CMT 10.19.96
31.79	131.63	−53.0	20.0	0.006	−43.5	CMT 5.2.96
31.79	131.31	−53.4	15.0	0.011	−43.3	CMT 12.2.96
31.73	131.59	−41.2	20.0	0.006	−43.6	CMT 10.19.96
31.29	131.29	−44.4	15.0	0.010	−44.0	CMT 12.16.98
30.59	131.24	−46.6	20.0	0.005	−44.9	CMT 9.14.79
30.59	131.07	−59.8	15.0	0.010	−44.8	CMT 11.11.96
29.78	130.51	−49.4	20.0	0.005	−45.5	CMT 7.24.95
29.77	130.63	−41.7	20.0	0.005	−45.6	CMT 6.2.86
29.48	130.64	−46.6	20.0	0.005	−46.0	CMT 9.27.98
29.28	130.31	−44.0	20.0	0.005	−46.0	CMT 10.17.99
29.26	129.86	−43.8	20.0	0.005	−45.8	CMT 9.13.94
29.24	130.31	−35.0	20.0	0.005	−46.1	CMT 1.23.84
29.20	130.31	−45.8	20.0	0.005	−46.1	CMT 3.1.85
28.51	130.00	−46.6	20.0	0.004	−46.8	CMT 3.24.86
27.99	129.39	−41.1	20.0	0.004	−47.0	CMT 11.20.89
27.52	128.44	−40.0	20.0	0.004	−47.0	CMT 1.15.95
27.48	128.57	−48.0	15.0	0.007	−47.1	Seno *et al.* (1993)
27.42	128.48	−45.4	20.0	0.004	−47.1	CMT 6.2.96
26.61	127.81	−51.4	20.0	0.004	−47.6	CMT 5.17.90
24.88	125.33	−42.3	20.0	0.003	−47.9	CMT 8.29.78
24.30	125.21	−43.0	10.0	0.013	−48.4	Seno *et al.* (1993)
24.24	125.23	−55.1	20.0	0.003	−48.5	CMT 9.30.90

Table 1b. Data at the PA-PH boundary (Izu-Bonin Trench).

Lat. (°N)	Lon. (°E)	Obs. (deg)	σ (deg)	IMP	Pre. (deg)	Source or reference
35.93	140.08	−89.0	15.0	0.019	−82.9	Seno *et al.* (1993)
35.86	141.35	−64.6	20.0	0.012	−80.9	CMT 1.9.95
35.76	140.70	−83.0	15.0	0.020	−81.9	Seno *et al.* (1993)
35.74	141.08	−75.5	20.0	0.012	−81.3	CMT 8.6.91
35.68	140.65	−84.3	20.0	0.011	−82.0	CMT 3.17.89
35.67	140.64	−80.0	15.0	0.020	−82.0	Seno *et al.* (1993)
35.58	140.61	−75.3	20.0	0.011	−82.0	CMT 12.30.83
35.57	140.65	−68.6	20.0	0.011	−82.0	CMT 12.30.83
35.56	140.54	−92.4	20.0	0.011	−82.1	CMT 3.6.89
34.02	141.63	−86.0	10.0	0.053	−80.1	Seno *et al.* (1993)
33.91	141.35	−94.4	20.0	0.013	−80.5	CMT 9.19.84
33.61	141.71	−78.0	10.0	0.054	−79.8	Seno *et al.* (1993)
33.49	141.40	−90.9	20.0	0.013	−80.3	CMT 10.27.98
33.38	140.97	−80.0	20.0	0.013	−81.0	Seno *et al.* (1993)
33.31	141.36	−91.6	20.0	0.014	−80.4	CMT 12.14.79
33.26	141.34	−75.6	15.0	0.024	−80.4	CMT 3.23.99
32.61	141.27	−79.8	20.0	0.014	−80.3	CMT 8.14.92
31.35	140.96	−82.3	20.0	0.015	−80.6	CMT 6.11.92
31.34	141.80	−80.0	15.0	0.028	−79.1	Seno *et al.* (1993)
31.22	141.75	−89.2	20.0	0.016	−79.2	CMT 5.29.92
31.11	142.09	−82.0	10.0	0.065	−78.5	Seno *et al.* (1993)
30.92	141.51	−93.8	20.0	0.016	−79.5	CMT 8.22.94
30.75	141.73	−72.0	10.0	0.065	−79.1	Seno *et al.* (1993)
30.71	141.82	−72.0	15.0	0.029	−78.9	Seno *et al.* (1993)
30.69	141.62	−86.3	15.0	0.029	−79.2	CMT 5.30.92
30.63	141.63	−88.8	20.0	0.016	−79.2	CMT 5.31.92
30.61	141.62	−90.2	20.0	0.016	−79.2	CMT 4.16.86
29.34	142.23	−75.0	10.0	0.074	−77.7	Seno *et al.* (1993)
29.31	141.98	−90.4	20.0	0.018	−78.2	CMT 5.14.98
29.30	142.02	−81.2	20.0	0.018	−78.1	CMT 12.16.88
28.97	142.05	−87.5	20.0	0.019	−77.9	CMT 9.12.99
28.12	142.41	−89.2	20.0	0.020	−77.0	CMT 1.11.81
27.84	142.76	−78.0	15.0	0.038	−76.2	Seno *et al.* (1993)
27.72	142.08	−81.0	15.0	0.036	−77.5	Seno *et al.* (1993)
23.71	143.20	−70.0	10.0	0.122	−73.4	Seno *et al.* (1993)

The situation has been improving in recent years. Many new earthquake slip vectors have become available from the Harvard CMT catalogue references (Dziewonski *et al.* 1984a,b, 1985a,b, 1987a,b,c,d, 1988, 1989, 1990a,b, 1991a,b, 1992, 1993a,b, 1995, 1996a,b, 1997, 1998, 1999a,b,c, 2000a,b,c). The foundation of GPS observation networks makes rate data for the Philippine Sea plate available. Hence it is now possible to determine the Euler vector of the Philippine Sea plate more accurately. In this study, we determine a new PH–PA Euler vector with a global inversion using more slip vectors, GPS data, and the 1122 data from the NUVEL-1 model (DeMets *et al.* 1990) and the NUVEL-1A model (DeMets *et al.* 1994), respectively.

Method of determining the Euler vector of the Philippine Sea plate

Although the NUVEL-1A global plate motion model gives Euler vectors for 13 plates, that for the Philippine Sea plate was just taken from the results of Seno *et al.* (1987, 1993) rather than being obtained from the global inversion owing to the limited data. In this study, we add the Philippine Sea plate to the 12 plates in the NUVEL-1 and NUVEL-1A models, respectively, and determine the Euler vectors of all 13 plates, respectively, by a global inversion, such that all are constrained within a global plate circuit closure. The inversion method used in this study is the same as that used by DeMets *et al.* (1990), which is an iterative linearized, weighted, least-squares procedure (Chase 1972; Minster *et al.* 1974). To obtain the NUVEL-1A model, DeMets *et al.* (1994) have simply modified NUVEL-1 model by multiplying by 0.9562 all of the rotation rates of 12 Euler vectors according to the changing of the opening rate data. In this study, we multiply by 0.9562 all the rate data in NUVEL-1 and treat them as rate data in NUVEL-1A and use these data for inversion to obtain the Euler vectors in the NUVEL-1A model.

Data and the selection principles

We must take into account the complication along the boundary areas of PH as discussed in introduction when we select the data. Three data sets were used in this study.

(1) The 1122 data, consisting of spreading rates, transform fault azimuths, and earthquake slip vectors, from NUVEL-1 model (DeMets *et al.* 1990) and NUVEL-1A model (DeMets *et al.* 1994), respectively. The rate data in NUVEL-1A model we mention here are those in NUVEL-1 multiplied by 0.9562 as suggested by DeMets *et al.* (1994).

(2) Earthquake slip vectors along the Philippine Sea plate boundaries. We discard slip vectors in the Luzon Trough–Philippine Trench because the Philippine Archipelago is a complicated deformation zone with a nearly N–S striking, left-lateral strike-slip fault passing through it (Barrier *et al.* 1991), which makes the relative

Table 2. Velocities of GPS stations relative to Eurasia plate.

GPS	Lat.	Lon.	Rate (mm yr^{-1})					Azimuth (deg)					
station	(°N)	(°E)	Obs.	σ (mm yr^{-1})	IMP	Pre.	Seno *et al.* (1993)	Obs.	σ (deg)	IMP	Pre.	Seno *et al.* (1993)	Note
S063	22.67	121.47	68.60	4.0	0.283	71.55	74.30	314.6	3.0	0.313	312.15	308.91	1
S102	22.04	121.56	71.70	1.5	0.515	72.20	75.03	316.8	2.0	0.293	311.59	308.37	2
BTS3	20.44	121.96	80.70	2.5	0.202	73.69	76.73	298.6	3.0	0.113	310.11	306.94	2
Okin.	20.43	136.08	59.77	13.5	0.010	61.21	64.79	300.1	13.0	0.024	300.02	296.25	3
Guam	13.59	144.87	22.52	3.0		66.16	71.02	301.0	7.0		286.81	283.72	4
Palau	7.34	134.48	100.42	10.0		80.72	85.48	277.9	6.0		293.	291.08	4

Note: (1) computed from Yu *et al.* (1999); Yu *et al.* (1997); (2) Yu *et al.* (1999); (3) Kato *et al.* (1996); (4) computed from Kato *et al.* (1998).

Table 3. Information distribution.

	Rate (GPS)	Azimuth		Total
		GPS	Slip vector	
EU–PH	1.012 25	0.749 33	0.283 53	2.045 11
PA–PH			0.965 80	0.965 80
Total	1.012 25	0.749 33	1.249 33	3.010 91

motion between EU and PH more complicated. We do not use the data on the Mariana Trench because of the approximate 40 mm yr^{-1} spreading at the Mariana backarc basin (Hussong & Uyeda 1981), which may affect the coupling between PH and PA. Also we discard the slip vectors along the North America (NA)–PH boundary, because the data have large uncertainties (Seno *et al.* 1993). Although the plate boundary has been discussed in light of the recent

Table 4. Comparison of Euler vectors from this study and NUVEL-1 (Pacific fixed).

No	Plate name	Lat. of pole (°N)		Lon. of pole (°E)		Rotation rate (deg Myr^{-1})	
		Ours	NUVEL-1	Ours	NUVEL-1	Ours	NUVEL-1
01	N. America	48.82	48.71	−77.87	−78.17	0.782	0.783
02	Cocos	36.86	36.82	−108.59	−108.63	2.089	2.089
03	Nazca	55.65	55.58	−89.97	−90.10	1.421	1.422
04	Antarctica	64.44	64.32	−83.72	−83.98	0.910	0.909
05	S. America	55.15	55.00	−85.30	−85.75	0.665	0.666
06	Eurasia	61.18	61.07	−85.56	−85.82	0.897	0.899
07	Africa	59.25	59.16	−72.82	−73.17	0.969	0.970
08	Caribbean	54.25	54.20	−80.48	−80.80	0.852	0.853
09	Australia	60.01	60.08	1.89	1.74	1.125	1.123
10	Arabia	59.62	59.66	−33.20	−33.19	1.162	1.162
11	India	60.44	60.49	−30.44	−30.40	1.154	1.154
12	Philippine	2.38	−1.24*	−44.54	−45.81*	0.961	1.000*

*From Seno *et al.* (1993).

Table 5. Comparison of Euler vectors from this study and NUVEL-1A (Pacific fixed).

No	Plate name	Lat. of pole (°N)		Lon. of pole (°E)		Rotation rate (deg Myr^{-1})	
		Ours	NUVEL-1A	Ours	NUVEL-1A	Ours	NUVEL-1A
01	N. America	48.84	48.71	−77.85	−78.17	0.748	0.749
02	Cocos	36.88	36.82	−108.61	−108.63	1.994	1.998
03	Nazca	55.70	55.58	−89.93	−90.10	1.359	1.360
04	Antarctica	64.45	64.32	−83.65	−83.98	0.870	0.870
05	S. America	55.15	55.00	−85.21	−85.75	0.636	0.637
06	Eurasia	61.19	61.07	−85.54	−85.82	0.857	0.859
07	Africa	59.26	59.16	−72.79	−73.17	0.927	0.927
08	Caribbean	54.21	54.20	−80.42	−80.80	0.814	0.816
09	Australia	60.00	60.08	1.89	1.74	1.077	1.074
10	Arabia	59.62	59.66	−33.13	−33.19	1.112	1.111
11	India	60.46	60.49	−30.31	−30.40	1.104	1.103
12	Philippine	−0.11	−1.24*	−44.34	−45.81*	0.961	1.000*

*From Seno *et al.* (1993).

Table 6. Some Euler vectors and comparision with Seno *et al.* (1993).

Plate pair	Lat. of pole (°N)			Lon. of pole (°E)			Rotation rate (deg Myr^{-1})		
	Ours		Seno *et al.* 1993	Ours		Seno *et al.* (1993)	Ours		Seno *et al.* (1993)
	N_1	N_1A		N_1	N_1A		N_1	N_1A	
PH–PA	2.38	−0.11	−1.24	−44.34	−43.85	−45.81	0.961	0.964	1.000
EU–PH	46.99	46.67	48.23	159.83	158.90	156.97	1.020	1.035	1.085
CR–PH	5.00	6.20	6.24	135.10	134.20	134.09	0.300	0.400	0.700
PA–CR	−5.71	−4.18	−10.13	135.91	137.52	134.43	0.665	0.568	0.309

N_1 and N_1A denote our results consistent with NUVEL-1 and NUVEL-1A, respectively.

GPS data, it is possible that Northern Honshu is part of the Okhotsk plate (Wei & Seno 1998).We use only the slip vectors along the Nankai Trough–Ryukyu Trench at the EU–PH boundary, and along the Izu–Bonin Trench at the PA–PH boundary.

To make sure that the slip vectors represent the direction of interplate motion, we choose them according to three rules. First, we use earthquakes with a scalar moment of 10^{24} dyn cm or more. Secondly, we required that the hypocentres appear to be located in the subduction zone and on the top surface of the Benioff zone. Ten cross-sections have been used to determine the hypocentre locations on the subduction zone. Fig. 1(a) shows the locations of the earthquakes chosen and cross-sections used to choose the earthquakes; Fig. 1(b) shows two cross-sections (cross sections 3 and 8 in Fig. 1a). Thirdly, we require that the depths of hypocentres are between 15 and 60 km, the fault plane solutions show thrust faulting, and the dip of the fault planes are close to the dip of the Wadati–Benioff zone. Finally, we choose 30 earthquake slip vectors at Nankai Trough–Ryukyu Trench and 35 at Izu–Bonin Trench, including 23 from Seno *et al.* (1993). Two of the slip vectors used by Seno *et al.* (1993) were not used here according to the principle of data selection in this study. One data point (33.76°N, 137.20°E) from Katsumata & Sykes (1969) has a depth of 21 km and a fault strike of 267.5°, which differs significantly from the trench strike. The second earthquake (31.14°N, 131.33°E) comes from Fitch (1972), and has a depth of 8 km, which is too shallow and may have a greater error. Table 1 gives these slip vectors, their errors and data importance, and their predicted values from this study.

(3) Velocities of PH relative to the EU from GPS observation. Some velocities of the PH relative to the EU are given in Table 2, which are from the Taiwan GPS Network (Yu *et al.* 1997, 1999) and the western Pacific integrated network (Kato *et al.* 1996, 1998). The velocities at station S102 and BTS3 are taken from Yu *et al.* (1997) directly. The velocity at station Okino Torishima (Okin.) is taken from Kato *et al.* (1996). The velocities at stations Guam and Palau are taken from Kato *et al.* (1998), but they give the velocities in the E–W component (V_{EW}) and the N–S component (V_{NS}). We made a simple calculation to obtain the magnitude of velocity from V_{EW} and V_{NS} relative to stable Eurasia. Yu *et al.* (1999) obtained the velocity at permanent station S01R relative to stable Eurasia and Yu *et al.* (1997) gave the velocity at station S063 relative to S01R, which is located on the volcanic island of Lutao. We calculate the velocity at station S063 relative to stable Eurasia from the data of Yu *et al.* (1997, 1999) and consider the propagation of the uncertainties. Yu *et al.* (1999) and Kato *et al.* (1996, 1998) referenced their velocities to a Eurasia fixed reference frame defined by very long baseline interferometry (VLBI) (Heki 1996). Yu *et al.* (1999) tied their velocities to Shanghai, Kato *et al.* (1996, 1998) tied their velocities to the station velocity at Tsukuba. Heki's result was derived using VLBI data from eastern Asia and western Europe and his velocities of Shanghai and Tsukuba with respect to the stable part of the Eurasia plate have been confirmed by recent GPS studies (e.g. Shen *et al.* 2000). In this study, for the four velocities we use, three are from Yu *et al.* (1997, 1999) and are referenced to a VLBI velocity at Shanghai and one from Kato *et al.* (1996), which is referenced to a VLBI velocity at Tsukuba. Because the two reference sites involved are about 2000 km apart from each other, we feel that the reference of our network should be fairly robust. Data from the Guam and Palau GPS stations are not used for the inversion, for reasons discussed briefly below. We used four GPS stations, S063, S102, BTS3 and Okino Torishima in the global inversion. Table 2 also shows the IMP for the data in the four stations.

Table 3 shows the information distribution for the data sets used in this study. It can be seen that the cumulative data importance for the four GPS velocities is 1.7616 and 1.2493 for slip vectors around PH boundaries, and the total cumulative data importance for PH is 3.010 91. So the four GPS velocities supply the majority of information concerning PH motion.

RESULTS

Tables 4 and 5 show the Euler vectors of the 12 plates relative to the Pacific plate obtained by inverting all the data simultaneously, subject to global plate circuit closure. The results in Tables 4 and 5 come from different spreading rate data from NUVEL-1 and NUVEL-1A, respectively. The results of the NUVEL-1 (DeMets *et al.* 1990) and the NUVEL-1A (DeMets *et al.* 1994) model are also given for comparison. The corresponding EU–PH and PA–PH Euler vectors are shown in Table 6. Fig. 2 shows the locations of the PA–PH and EU–PH Euler poles of this study and previous studies.

In addition to these major plates, the region may contain several microplates. Of these, the proposed Caroline Plate has the most important influence on our estimate of the Euler vector for the Philippine Sea plate. The boundary constraints for PA–CR motion: divergence at the Sorol Trough and convergence at the Mussau Trench, both of which would be on the boundary, were proposed by Weissel & Anderson (1978). We followed earlier studies and used these constraints. We obtained our PA–PH Euler vector from the global inversion and then adjusted the CR–PH Euler vector, to obtain a set of PA–CR Euler vectors satisfying the PA–CR boundary constraints. Table 6 shows the result of PA–PH, EU–PH, CR–PH Euler vectors and a PA–CR Euler vector that can satisfy the PA–CR boundary constraints and predict the most obvious spreading along the PA–CR boundary. The results of Seno *et al.* (1993) are also shown.

Seno *et al.* (1993) have adjusted the PA–PH Euler vector to satisfy the PA–CR boundary constraints. They have obtained its pole and found that only rotation rates $\leq 0.7^\circ$ Myr^{-1}could satisfy the CR–PH constraints. We found that the rotation rate of the CR–PH Euler vector must be less than 0.5° Myr^{-1} if a PA–CR Euler vector satisfies

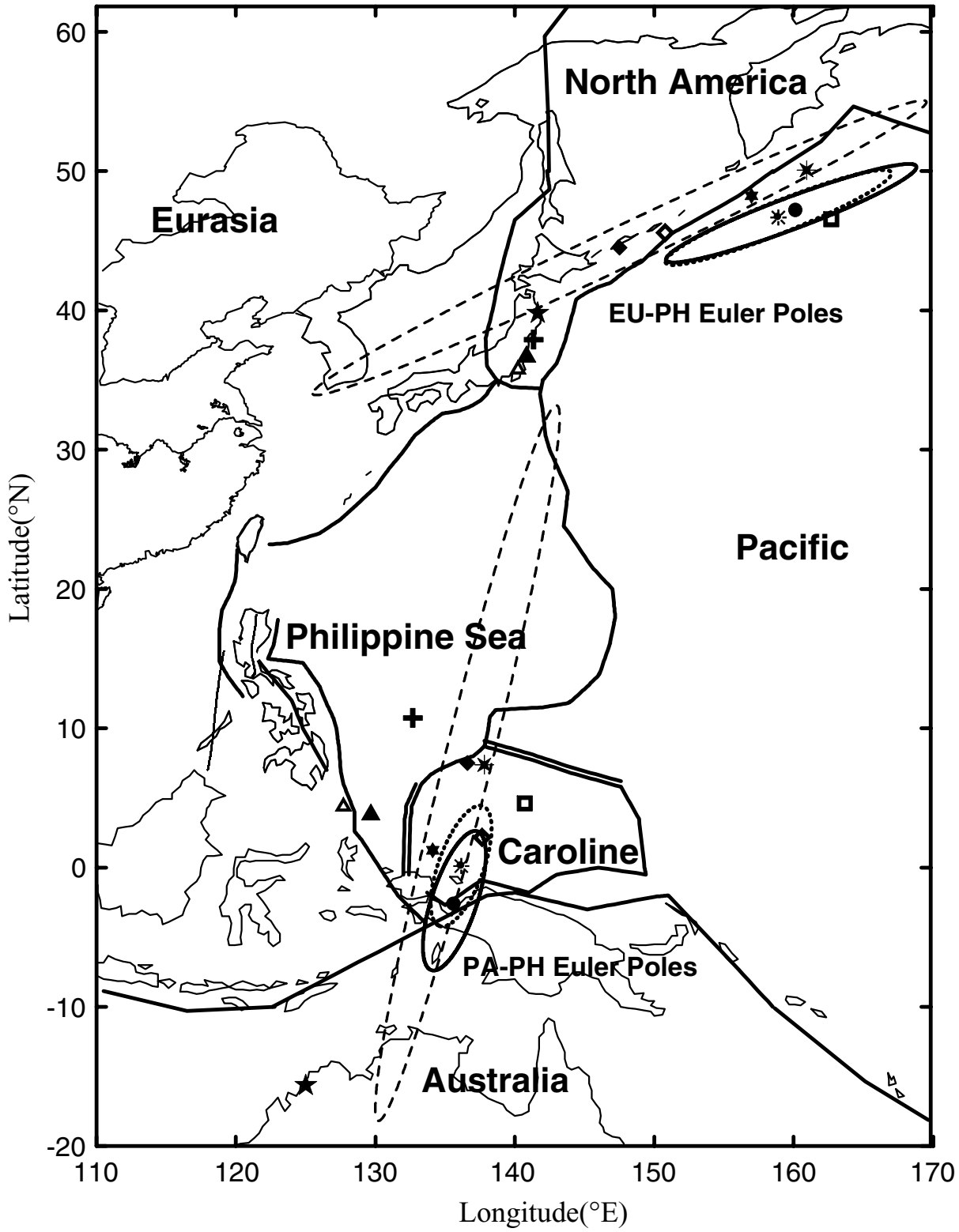

Figure 2. Euler poles of EU–PH and PA–PH from different researchers. Solid line ellipses and dotted line ellipses are the 95 per cent confidence error ellipses found in this study consistent with NUVEL-1 and NUVEL-1A, respectively, and the dashed line ellipses are the 68 per cent confidence error ellipses of best-fitting poles from Seno *et al.* (1993). •, this study (consistent with NUVEL-1); *, this study (with NUVEL-1A); ⋆, Chase (1978); □, Minster & Jordan (1978); △, Karig (1975); +, Huchon (1986); ▲, Ranken *et al.* (1984); ◇, Seno (1977); ♦, Seno *et al.* (1993) best-fitting pole; black six-pointed star, Seno *et al.* (1993); black four-pointed star with cross, this study using only earthquake slip vectors. Plate name abbreviations; EU, Eurasia; PH, Philippine Sea; PA, Pacific; NA, North America; CR, Caroline; AU, Australia. **Au: please check, symbols are not clear**

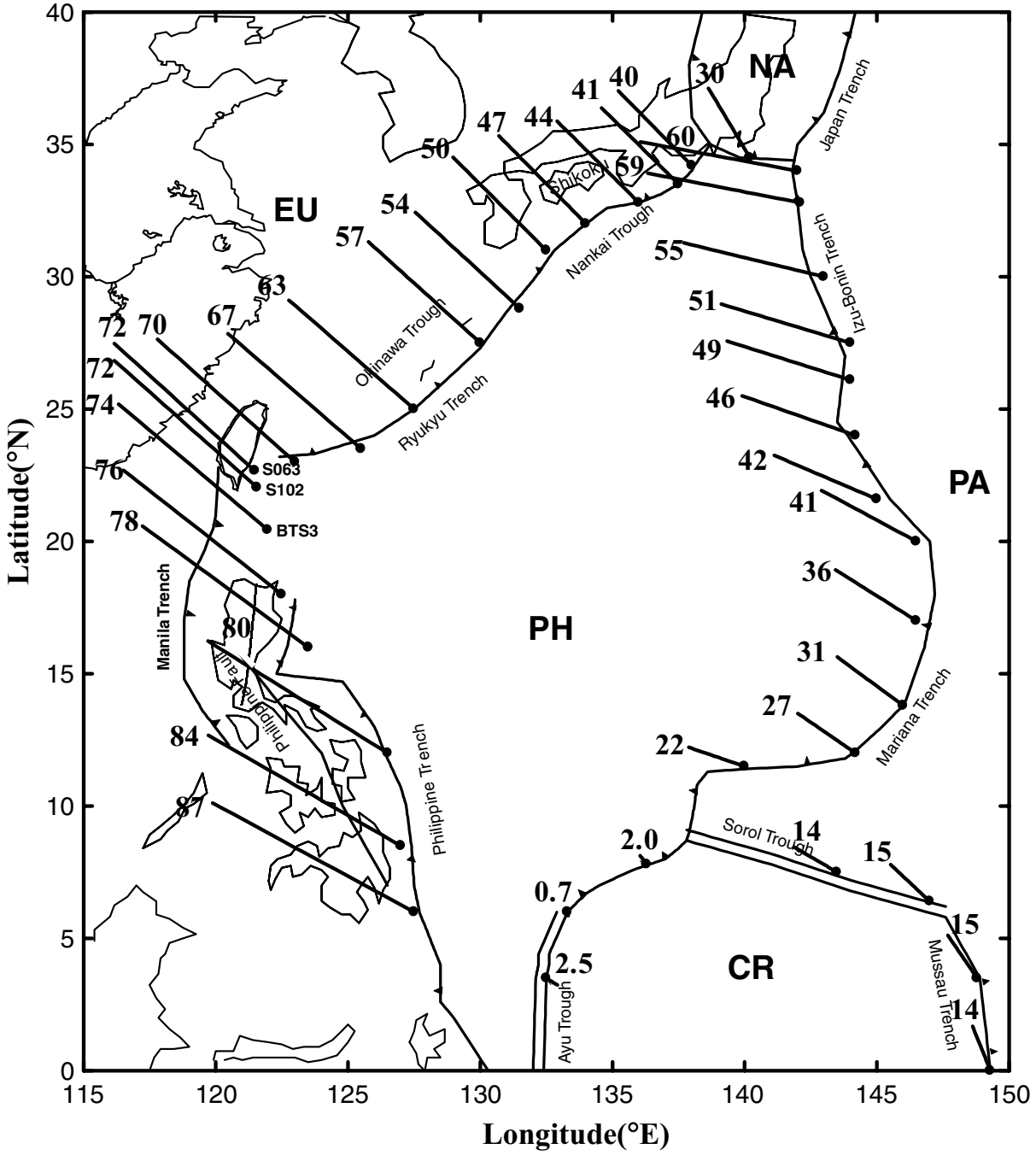

Figure 3. Relative velocities around PH and CR. Along the EU–PH and NA–PH boundaries, PH motions with respect to EU or NA are shown; along the PA–PH and PA–CR boundaries, PA motions with respect to PH or CR are shown; and along the CR–PH boundary, CR motions with respect to PH are shown. Azimuths are indicated by bars directed from circles.

the PA–CR boundary constraint. Fig. 3 shows the relative velocities around PH and CR for our study consistent with the NUVEL-1A model.

DISCUSSION AND CONCLUSION

Comparison of the observed data and the predicted results

From Tables 4 and 5 we can see that the change of opening rate data has a much greater influence on the poles of the Philippine sea plate than that of the others, and the rotation rates of the other 11 plates for the NUVEL-1A model can be well determined by multiplying the rotation rates of the NUVEL-1 model by, but the poles are not exactly the same. We mainly use the results consistent with NUVEL-1A model for the discussion below.

We discuss the consistency of the observed data and the predicted values at the Philippine Sea plate boundaries. The results of Seno *et al.* (1993) are also included for comparison.

First, we compare the azimuths of earthquake slip vectors. The results from two global inversions are very similar, but we only give

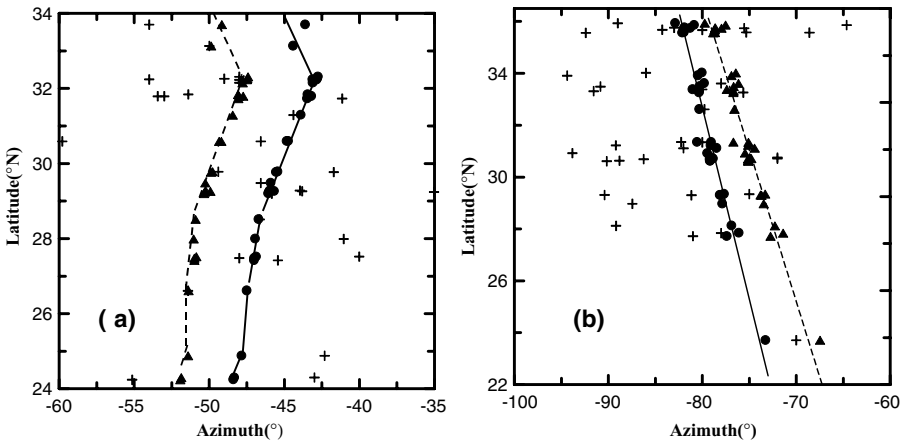

Figure 4. Compaison of the predicted and observed azimuths of earthquake slip vectors. (a) Nankai Trough–Ryukyu Trench, the PH–EU boundary. (b) Izu–Bonin Trench, the PA–PH boundary. Crosses denote observed data; black dots denote values predicted by this study; triangles are the predicted value from Seno *et al.* (1993); the lines through the points are just to guide the eye.

the result consistent with NUVEL-1A. Figs 4(a) and (b) show the comparison of the observed and the predicted azimuths at the Nankai Trough–Ryukyu Trench along the PH–EU boundary, and the Izu–Bonin Trench along the PA–PH boundary. The predicted values are basically more consistent with the observed data and slight better than those of Seno *et al.* (1993). We think that Seno's adjustment of the PA–PH Euler pole inside the 68 per cent confidence error ellipse in order to gain a PA–CR Euler vector satisfying the PA–CR constraint reduced the fit to the observed slip vectors at the PA–PH boundary.

There is bias of the observed slip vectors from the predicted ones in the Nankai Trough as seen in Fig. 4(a). The misfit of the observed and predicted slip vectors is not very big, but is quite obvious. This may be caused by the deformation in the Shikoku area. The PH subducted beneath southwest Japan and the MTL passes through southwest Japan, according to Le Pichon *et al.* (1998). On one hand, the right-hand strike-slip motion is about 10–15 mm yr^{-1} along the MTL, and it should produce an elastic deformation in the area between MTL and the Nankai Trough. The deformation causing elastic motion in the SWW direction decreases gradually away from the MTL. On the other hand, the subduction of PH also causes elastic deformation of the crust of the overriding EU plate in the Shikoku area when the subducting PH is locked with EU, its direction should be NW, coincident with that of subduction (Le Pichon *et al.* 1998; El-Fiky & Kato 1999). The average rate is about 43 $\pm$ 5 mm yr^{-1} (El-Fiky & Kato 1999). The resultant elastic motion should be in a direction between NW and SWW, it depends upon the magnitudes of the two kinds of motion. Thus, focal mechanism solutions may diverge from the direction of subduction or PH motion. We cannot make a quantitative calculation, but this intraplate deformation may explain the fact that the observed slip vectors are systematically more westwards than the predicted one (Fig. 4a). Let us make a rough estimate: the elastic motion near the Nankai Trough caused by the relative motion along MTL is smaller than 10–15 mm yr^{-1}, we suppose it is 10 mm yr^{-1} and in the SWW direction. The elastic motion near the Nankai Trough caused by subduction of PH is about 43 mm yr^{-1} (El-Fiky & Kato 1999), we assume it is 40 mm yr^{-1} in the NW direction. So the difference between the observed and predicted value is less than 12°, it seems to fit the result in Fig. 4a.

The Okinawa Trough is rifting gradually from south to north (Miki *et al.* 1990). Imanishi *et al.* (1996) obtained the opening rate in the southern part of the Okinawa Trough using GPS data. The opening rate is about 33.3 mm yr^{-1} at Hate station, 29.1 mm yr^{-1} at Ishi station and 19.8 mm yr^{-1} at Niya station. The opening rate decreases from south to north and the direction of the opening velocities is nearly parallel to the subduction direction of PH. In this study only the orientation of earthquake slip vectors were used and most of the earthquakes are located to the north of those GPS stations. So the slip vectors are insensitive to the opening of the Okinawa Trough.

The predicted (consistent with NUVEL-1A) and observed values of GPS data, indicated by solid and dashed bars with arrows, respectively, are shown in Fig. 5. The velocities at the GPS stations predicted by this study and Seno *et al.* (1993) are listed in Table 2. The predicted and observed velocities agree well at station S063, S102 and Okino Torishima, especially the Okino Torishima station, which has an observed velocity (59.77 mm yr^{-1}, $-59.9°$N) and a predicted velocity (61.48 mm yr^{-1}, $-59.4°$) from this study (Fig. 5 and Table 2). The consistency between the observed and predicted values is better than for Seno *et al.* (1993), which give a slight but larger misfit (Kato *et al.* 1996).

Among the four GPS stations we used in the inversion, the misfit between the observed and predicted values of BTS3 is relatively high. It seems that BTS3 is far from the Taiwan collision zone. Therefore, its motion could be more representative of the Philippine plate motion than S063 and S102 because S063 and S102 are closer to the Taiwan collision zone, but the effect of the collision on S063 and S102 is probably minor, as can be seen from Table 2. The observed velocities at the two stations are slightly smaller than that predicted by this study and Seno *et al.* (1993) (they did not use the GPS velocities in their study). BTS3 is far from the Taiwan collision zone, but it is within the deformation zone between Taiwan and Luzon, and close to the extension of PF to the west. Thus it can be affected by the deformation there (Zang *et al.* 1994). Luzon Island is between the east-dipping subduction of the South China Sea oceanic basin and the west-dipping subduction along East Luzon Trough and the Philippine Trench. The left-lateral strike-slip PF extends near the N–S direction through Luzon island.

Recently, Yu *et al.* (1999) studied the crustal deformation in the Taiwan–Luzon region using the GPS data from 1996 to 1998. They found that the PF system is very active; the left-lateral slip is from

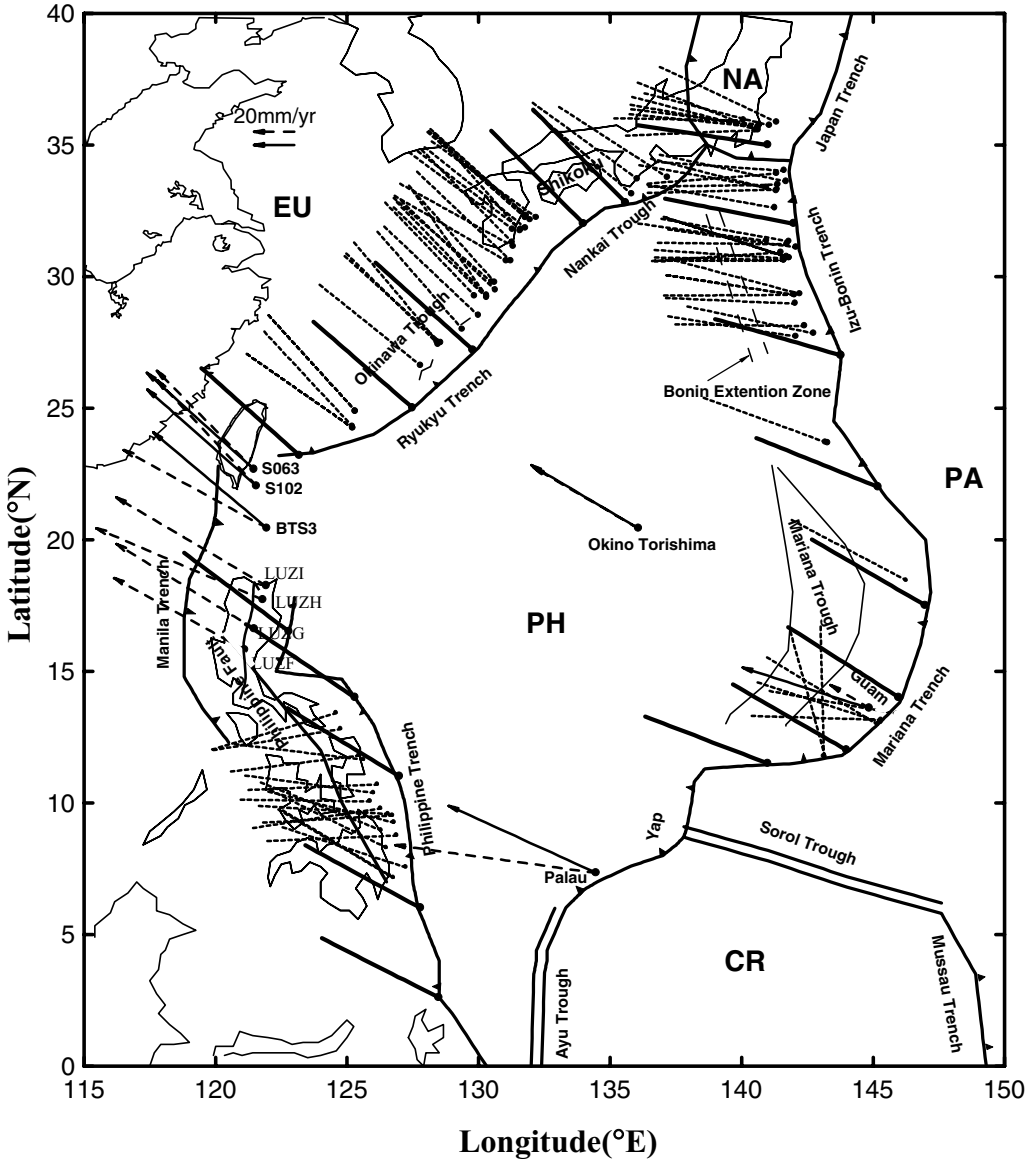

Figure 5. Comparison of observed data and predicted values. Solid dots indicate locations of data. Dashed bar along PH-EU and PA-PH boundaries represent the azimuth of earthquake slip vector while the bold solid bar represent the predicted azimuth of relative motion at the two boundaries. Solid bar with arrow and dashed bar with arrow are the predicted and observed velocity vector of GPS station relative to the Eurasia plate, respectively. Scale on top-left corner measures magnitudes of GPS velocity vectors only.

17 to 31 mm yr^{-1} and the convergence rate is from 7 to 15 mm yr^{-1} in the northern and eastern parts of Luzon. Table 7 shows the velocities of GPS stations to the east of PF and in central and northern Luzon relative to stable Eurasia. The velocity at BTS3 is also shown for comparison. The velocities were calculated in the same way as stations S102 and S063 (Fig. 5). It can be found that the stations to the east of the PF have a similar azimuth as the velocities but the rate of velocities increases from northern Luzon to central Luzon and then decreases to the south. The velocity at GPS station BTS3 is closer to that at stations on Luzon Island than that in the Taiwan region, so it has quite a strong influence from the deformation of the Philippine archipelago.

Table 7. Velocities of GPS stations to the east of PF relative to stable Eurasia.

Station	Lat. (deg)	Long. (deg)	V (mm yr^{-1})	Azimuth (deg)
S063	22.666	121.470	68.6 ± 4.0	315.4 ± 3.0
S102	22.037	121.558	71.7 ± 1.5	316.8 ± 2.0
BTS3	20.438	121.963	80.7 ± 2.5	298.6 ± 2.0
LUZI	18.246	121.928	86.2 ± 2.7	300.5 ± 2.0
LUZH	17.717	121.804	89.6 ± 3.0	293.2 ± 2.0
LUZG	16.608	121.482	80.1 ± 2.7	301.6 ± 2.0
LUZF	15.815	121.113	73.8 ± 2.4	298.8 ± 2.0

PF is the Philippine Fault.

Deformation inside the Philippine Sea plate and along the plate boundaries

The predicted and the observed motions agree well at the Nankai Trough–Ryukyu Trench and Izu–Bonin Trench (Fig. 5). Similarly, so do the predicted and observed results at GPS stations S063, S102 and Okino Torishima. The consistency shows that these areas move

uniformly as a rigid plate. At the Philippine Trench, Mariana Trough and Yap–Palau Trench, the predicted and observed results show poor consistency, implying that our decision not to use these data in the inversion may have been wise.

The Guam GPS station lies between the Mariana Trench and the Mariana Trough. It shows significant misfit between the observed and predicted azimuth and rate of motion relative to Eurasia. The misfit of the rate is about 40 mm yr^{-1} and the direction is nearly E–W (Fig. 5). This misfit is consistent with the spreading rate of the Mariana Trough given by Hussong & Uyeda (1981). The misfit between predicted and observed results at Palau station is also obvious. This may be a result of Palau station being close to the Caroline Plate subduction boundary.

In the Philippine Trench, the predicted and observed results also show poor consistency, which may be caused by motion along the sinistral PF in decoupling the Philippine Archipelago (Seno 1977; Seno & Kurita 1978) from the Philippine Sea plate and the interplate deformation of the Philippine Archipelago (Cardwell *et al.* 1980; Zang *et al.* 1994). One reason for the interplate deformation is possibly that the South China Sea is moving eastward at about 10 mm yr^{-1} with respect to Eurasia (Molnar & Gipson 1996) and its subduction beneath the Philippine archipelago in a nearly EW direction along the Manila Trench may cause deformation in the Philippine archipelago, including elastic deformation in the EW direction (Zang *et al.* 1994). This elastic deformation will cause movement in the EW direction when a big intraplate earthquake occurs in the Philippine Trench, the direction of the resultant movement caused by the interplate earthquake will be different from the direction of the subduction of PH in the Philippine Trench and becomes more westward than the direction of subduction of PH—this may cause the poor consistency between the observed slip vectors and the predicted one.

ACKNOWLEDGMENTS

We are grateful to Dr T. Kato at the Earthquake Institute of Tokyo University and Dr Shui-Beih Yu at the Earth Sciences Institute in Taiwan for their new prints and GPS data. We thank Professor Seth Stein for his reviewing and correcting of the manuscript. We would like to thank the two reviewers for their comments and suggestions that were invaluable in improving the manuscript. This research was supported by the key project of 'mechanism and prediction of continental strong earthquake' under grant 95-13-04-06, and 'natural science foundation of China' under grant 49874020.

REFERENCES

Barrier, E., Huchon, P. & Aurelio, M., 1991. Philippine Fault—a key for philippine kinematics, *Geology,* **19**, 32–35.

Cardwell, R.K., Isacks, B.L. & Karing, D.E., 1980. The spatial distribution of earthquakes, focal mechanism solutions, and subducted lithosphere in the Philippine and northeasten Indonesian Islands, *Geophys. Monogr. Amer. Geophys. Union,* **23**, 1–35.

Chase, C.G., 1972. The, *N* plate problem of plate tectonics, *Geophys. J. R. astr. Soc.,* **29**, 117–122.

Chase, C.G., 1978. Plate kinematics: The Americas, East Africa, and the rest of the world, *Earth planet. Sci. Lett.,* **37**, 355–368.

DeMets, C., Gordon, R.G., Argus, D.F. & Stein, S., 1990. Current plate motions, *Geophys. J. Int.,* **101**, 425–478.

DeMets, C., Gordon, R.G., Argus, D.F. & Stein, S., 1994. Effect of recent revisions to the geomagnetic reversal time-scale on estimates of current plate motions, *Geophys. Res. Lett.,* **21**, 2191–2194.

Dziewonski, A.M., Franzen, J.E. & Woodhouse, J.H., 1984a. Centroid-moment tensor solutions for October–December 1983, *Phys. Earth planet. Inter.,* **34**, 129–136.

Dziewonski, A.M., Franzen, J.E. & Woodhouse, J.H., 1984b. Centroid-moment tensor solutions for January–March 1984, *Phys. Earth planet. Inter.,* **34**, 209–219.

Dziewonski, A.M., Franzen, J.E. & Woodhouse, J.H., 1985a. Centroid-moment tensor solutions for July–September 1984, *Phys. Earth planet. Inter.,* **38**, 203–213.

Dziewonski, A.M., Franzen, J.E. & Woodhouse, J.H., 1985b. Centroid-moment tensor solutions for January–March 1985, *Phys. Earth planet. Inter.,* **40**, 249–258.

Dziewonski, A.M., Ekstrom, G., Franzen, J.E. & Woodhouse, J.H., 1987a. Centroid-moment tensorsolutions for January–March 1986, *Phys. Earth planet. Inter.,* **45**, 1–10.

Dziewonski, A.M., Ekstrom, G., Franzen, J.E. & Woodhouse, J.H., 1987b. Centroid-moment tensorsolutions for April–June 1986, *Phys. Earth planet. Inter.,* **45**, 229–239.

Dziewonski, A.M., Ekstrom, G., Franzen, J.E. & Woodhouse, J.H., 1987c. Global seismicity of 1978, Centroid-moment tensorsolutions for 512 earthquakes, *Phys. Earth planet. Inter.,* **46**, 316–342.

Dziewonski, A.M., Ekstrom, G., Franzen, J.E. & Woodhouse, J.H., 1987d. Global seismicity of 1979, Centroid-moment tensorsolutions for 524 earthquakes, *Phys. Earth planet. Inter.,* **48**, 18–47.

Dziewonski, A.M., Ekstrom, G., Franzen, J.E. & Woodhouse, J.H., 1988. Global seismicity of 1981, Centroid-moment tensor solutions for 542 earthquakes, *Phys. Earth planet. Inter.,* **50**, 155–182.

Dziewonski, A.M., Ekstrom, G., Woodhouse, J.H. & Zwart, G., 1989. Centroid-moment tensor solutions for october december 1988, *Phys. Earth planet. Inter.,* **57**, 179–191.

Dziewonski, A.M., Ekstrom, G., Woodhouse, J.H. & Zwart, G., 1990a. Centroid-moment tensor solutions for January–March 1989, *Phys. Earth planet. Inter.,* **59**, 233–242.

Dziewonski, A.M., Ekstrom, G., Woodhouse, J.H. & Zwart, G., 1990b. Centroid-moment tensor solutions for October–December 1989, *Phys. Earth planet. Inter.,* **62**, 194–207.

Dziewonski, A.M., Ekstrom, G., Woodhouse, J.H. & Zwart, G., 1991a. Centroid-moment tensor solutions for April–June 1990, *Phys. Earth planet. Inter.,* **66**, 133–143.

Dziewonski, A.M., Ekstrom, G., Woodhouse, J.H. & Zwart, G., 1991b. Centroid-moment tensor solutions for July–September 1990, *Phys. Earth planet. Inter.,* **67**, 211–220.

Dziewonski, A.M., Ekstrom, G. & Salganik, M.P., 1992. Centroid-moment tensor solutions for July–September 1991, *Phys. Earth planet. Inter.,* **72**, 1–11.

Dziewonski, A.M., Ekstrom, G. & Salganik, M.P., 1993a. Centroid-moment tensor solutions for January–March 1992, *Phys. Earth planet. Inter.,* **77**, 143–150.

Dziewonski, A.M., Ekstrom, G. & Salganik, M.P., 1993b. Centroid-moment tensor solutions for July–September 1992, *Phys. Earth planet. Inter.,* **79**, 287–297.

Dziewonski, A.M., Ekstrom, G. & Salganik, M.P., 1995. Centroid-moment tensor solutions for July–September 1994, *Phys. Earth planet. Inter.,* **90**, 1–11.

Dziewonski, A.M., Ekstrom, G. & Salganik, M.P., 1996a. Centroid-moment tensor solutions for January–March 1995, *Phys. Earth planet. Inter.,* **93**, 147–157.

Dziewonski, A.M., Ekstrom, G. & Salganik, M.P., 1996b. Centroid-moment tensor solutions for July–September 1995, *Phys. Earth planet. Inter.,* **97**, 3–13.

Dziewonski, A.M., Ekstrom, G. & Salganik, M.P., 1997. Centroid-moment tensor solutions for April–June 1996, *Phys. Earth planet. Inter.,* **102**, 11–20.

Dziewonski, A.M., Ekstrom, G. & Maternovskaya, N.N., 1998. Centroid-moment tensor solutions for October–December 1996, *Phys. Earth planet. Inter.,* **105**, 95–108.

Dziewonski, A.M., Ekstrom, G. & Maternovskaya, N.N., 1999a. Centroid-moment tensor solutions for April–June 1998, *Phys. Earth planet. Inter.,* **112**, 11–19.

Dziewonski, A.M., Ekstrom, G. & Maternovskaya, N.N., 1999b. Centroid-moment tensor solutions for July–September 1998, *Phys. Earth planet. Inter.,* **114**, 99–107.

Dziewonski, A.M., Ekstrom, G. & Maternovskaya, N.N., 1999c. Centroid-moment tensor solutions for October–December 1998, *Phys. Earth planet. Inter.,* **115**, 1–16.

Dziewonski, A.M., Ekstrom, G. & Maternovskaya, N.N., 2000a. Centroid-moment tensor solutions for January–March 1999, *Phys. Earth planet. Inter.,* **118**, 1–11.

Dziewonski, A.M., Ekstrom, G. & Maternovskaya, N.N., 2000b. Centroid-moment tensor solutions for July–September 1999, *Phys. Earth planet. Inter.,* **119**, 311–319.

Dziewonski, A.M., Ekstrom, G. & Maternovskaya, N.N., 2000c. Centroid-moment tensor solutions for October–December 1999, *Phys. Earth planet. Inter.,* **121**, 205–221.

El-Fiky, G.S. & Kato, T., 1999. Interplate coupling in the Tohoku district, Japan, deduced from geodetic data inversion, *J. geophys. Res.,* **104**, 20 361–20 377.

Fitch, T.J., 1972. Plate convergence, transcurrent faults, and internal deformation adjacent to southeast Asia and the western Pacific, *J. geophys. Res.,* **77**, 4432–4457.

Heki, K., 1996. Horizontal and vertical crustal movements from three-dimensional very long baseline interferometry kinematic reference frame: implication for the reversal timescale revision, *J. geophys. Res.,* **101**, 3187–3198.

Huchon, P., 1986. Comments on 'Kinematics of the Philippine Sea plate' eds Ranken, B., Cardwell, R.K. & Karig, D.E., *Tectonics,* **5**, 165–168.

Hussong, D.M. & Uyeda, S., 1981. Tectonic processes and the history of the Mariana Arc: a synthesis of the results of deep sea drilling project Leg 60, *Initial Rep Deep Sea Drill Proj.,* **60**, 909–929.

Imanishi, M., Kimata, F., Inamori, N., Miyajima, R., Okuda, T., Takai, K., Hirahara, K. & Kato, T., 1996. Horizontal displacements by GPS Measurements at the Okinawa-Sakishima Islands (1994–1995), *J. seism. Soc. Japan,* **49**, 417–421.

Jarrard, R.D., 1986. Relations among subduction parameters, *Rev. Geophys.,* **24**, 217–284.

Karig, D.E., 1975. Basin genesis in the Philippine Sea, *Initial Rep Deep Sea Drill Proj.,* **31**, 857–879.

Kato, T., Kotake, Y., Chachin, T., Iimura, Y., Miyazaki, S., Kanazawa, T. & Suyehiro, K., 1996. An estimate of the Philippine Sea plate motion derived from the Global Positioning System observation at Okino Torishima, Japan, *J. Geod. Soc. Japan,* **42**, 233–243.

Kato, T. *et al.*, 1998. Initial results from WING, the continuous GPS network in the western Pacific area, *Geophys. Res. Lett.,* **25**, 369–372.

Katsumata, M. & Sykes, L.R., 1969. Seismicity and tectonics of the western Pacific: Izu–Mariana–Caroline and Ryukyu–Taiwan regions, *J. geophys. Res.,* **74**, 5923–5948.

Le Pichon, X., Francheteau, J. & Bonnin, J., 1976. Plate tectonics, 2nd edn, Elsevier, Amsterdam.

Le Pichon, X., Mazzotti, S., Henry, P. & Hashimoto, M., 1998. Deformation of the Japanese Islands and seismic coupling: an interpretation based on GSI permanent GPS observations, *Geophys. J. Int.* **134**, 501–514.

Miki, M., Matsuda, T. & Otofuji, Y., 1990. Opening mode of the Okinawa Trough–paleomagnetic evidence from the south ryukyu arc, *Tectonophysics,* **175**, 335–347.

Minster, J.B. & Jordan, T.H., 1978. Rotation vectors for the Philippine and Rivera plates, *EOS, Trans. Am. geophys. Un.,* **60**, 958.

Minster, J.B., Jordan, T.H., Molnar, P. & Haines, E., 1974. Numerical modelling of instantaneous plate tectonics, *Geophys. J. R. astr. Soc.,* **36**, 541–576.

Molnar, P. & Gipson, J.M., 1996. A bound on the rheology of continental lithosphere using very long baseline interferometry: the velocity of south China with respect to Eurasia, *J. geophys. Res.,* **101**, 545–553.

Morgan, W.J., 1971. Plate motions and deep mantle convection, in *Hess Volume,* ed. Shagam, R., *Geol. Soc. Am. Mem.,* p. 132.

Ranken, B., Cardwell, R.K. & Karig, D.E., 1984. Kinematics of the Philippine Sea plate, *Tectonics,* **3**, 555–575.

Seno, T., 1977. The instantaneous rotation vector of the Philippine Sea plate relative to the Eurasia plate, *Tectonophysics,* **42**, 209–226.

Seno, T. & Kurita, K., 1978. Focal mechanism and tectonics in the Taiwan–Philippine region, *J. Phys. Earth,* **26** (suppl.), S249–S263.

Seno, T., Moriyama, T., Stein, S., Woods, D.F., DeMets, C., Argus, D. & Gordon, R., 1987. Redetermination of the Philippine Sea plate motion (abstract), *EOS Trans. Am. geophysics Res.,* **68**, 1474.

Seno, T., Stein, S. & Gripp, A.E., 1993. A model for the motion of the Philippine Sea plate consistent with NUVEL-1 and Geological Data, *J. geophys. Res.,* **98**, 17 941–17 948.

Seno, T., Sakurai, T. & Stein, S., 1996. Can the Okhotsk plate be discriminated from the North American plate?, *J. geophys. Res.,* **101**, 11 305–11 315.

Shen, Z.K., Zhao, C.K., Yin, A., Li, Y.X., Jackson, D.D., Peng, F. & Dong, D., 2000. Contemporary crustal deformation in east Asia constrained by Global Positioning System measurements, *J. geophys. Res.,* **105**, 5721–5734.

Wei, D. & Seno, T., 1998. Determination of the American plate motion, in *Mantle Dynamics and Plate Interactions in Fast Asia,* Vol. 27, pp. 337–346, eds Flower, M. *et al., Geodynam, Am. geophys. Un. Monogr.*

Weissel, J.K. & Anderson, R.N., 1978. Is there Caroline Plate?, *Earth planet. Sci. Lett.,* **41**, 143–158.

Yu, S.B., Chen, H.Y. & Kuo, L.C., 1997. Velocity field of GPS station in the Taiwan area, *Tectonophysics,* **274**, 41–59.

Yu, S.B., Kuo, L.C., Punongbayan, R.S. & Ramos, E.G., 1999. GPS observation of crustal deformation in the Taiwan-Luzon region, *Geophysical Res. Lett.,* **26**, 923–926.

Zang, S.X., Chen, Q.Z. & Huang, J.S., 1994. Distribution of Earthquakes, Stress State and Interaction between Plates in Southern Taiwan–Philippine Area, *Seismogeol. Geol.*, **16**, 29–37(in Chinese).